Available online at www.sciencedirect.com
ScienceDirect
Journal of Nuclear Materials 361 (2007) 298–305
journal of nuclear materials
www.elsevier.com/locate/jnucmat

# Effect of severe ausforming via equal channel angular extrusion on the shape memory response of a NiTi alloy

B. Kockar [a], I. Karaman [a,*], A. Kulkarni [a], Y. Chumlyakov [b], I.V. Kireeva [b]

[a] Department of Mechanical Engineering, Texas A&M University, MS 3123, College Station, TX 77843, USA
[b] Siberian Physical Technical Institute, 634050 Tomsk, Russia

**Abstract**

The effects of severe plastic deformation via equal channel angular extrusion (ECAE) and cold drawing followed by low temperature annealing on the shape memory behavior of the $Ti_{50.27}Ni_{49.73}$ alloy were comparatively investigated. The ECAE billets were processed at 300 °C using a 90° angle ECAE tool while 30% cold drawing was performed at room temperature followed by a low temperature annealing treatment. Transformation temperatures, and transformation and irrecoverable strain levels were revealed using thermal cyclic experiments under various constant tensile stress levels. Considerable improvement in the thermal cyclic stability of transformation temperatures and transformation strains and reduction in irrecoverable strains under high stress levels were achieved in the ECAE processed material. More interestingly, the thermal hysteresis was notably lower in the ECAE case. This was attributed to the formation of favorable dislocation substructure and microstructural refinement due to the deformation twinning in austenite. The results showed that the severe ausforming via ECAE has certain advantageous over cold deformation followed by annealing process in enhancing the shape memory properties of NiTi alloys.


## 1. Introduction

NiTi alloys are the most popular shape memory alloys (SMAs) which show superior shape memory effect and pseudoelastic behavior as compared to Cu-based and Fe-based SMAs [1]. They have many technological applications in several areas including nuclear industry. NiTi SMAs can produce force upon phase transformation at moderate temperatures so that they can be utilized as actuators [2,3]. SMAs have already been used in the quick replacement technology for fusion reactors [3]. In such applications, NiTi SMA drivers function as a coupler for quick connection and disconnection of the main part and the core element with high neutron and thermal loading by controlling the SMA temperature [3]. The shape memory and mechanical properties of these alloys are highly dependant on thermomechanical treatments. Major thermomechanical treatments that have been reported in the literature are cold rolling, cold rolling followed by annealing, and severe plastic deformation (SPD) via high-pressure torsion (HPT) or equal channel angular extrusion (ECAE). ECAE is an innovative

* Corresponding author.
*E-mail address:* ikaraman@tamu.edu (I. Karaman).

0022-3115/$ - see front matter © 2006 Elsevier B.V. All rights reserved.
doi:10.1016/j.jnucmat.2006.12.007

processing technique which permits the application of large uniform strains without reduction in cross-section of the work piece [4]. In ECAE, the work piece passes through two intersecting channels with same cross-section and the intersection angle of usually 90° [4]. The extrusion of a billet through these channels produces simple shear at the channel intersection plane. More information about ECAE process can be found in [4,5]. The main advantages of ECAE over HPT are the possibility of processing much larger sample sizes and controlling the grain morphology and crystallographic texture [5]. It has been reported that NiTi alloys processed by SPD demonstrate high strength, ductility and superplasticity [6,7].

The effect of cold deformation and subsequent annealing on the phase transformation behavior of NiTi alloys has been extensively studied by Liu and his colleagues [8,9]. Miller et al. [10] studied the effect of cold deformation level and subsequent annealing temperature on the one-way and two-way shape memory response, and the thermomechanical behavior during thermal cycling under different stress levels. They found that transformation strain and the total plastic strain level decrease while the stress level for the onset of transformation-induced plasticity increases with the amount of cold work.

Several studies have been conducted on SPD of NiTi SMAs by Valiev and his colleagues [11,12] and Karaman et al. [13]. The former group investigated the nanocrystallization of amorphous NiTi processed by HPT as a result of subsequent annealing and reported an increase in the strength at failure up to 2650 MPa with an elongation to failure of 5% [11]. They have also utilized other SPD techniques such as ECAE, rolling and drawing with intermediate or subsequent annealing steps, and obtained ultrafine grained equiatomic NiTi alloys [14,15]. However, they only investigated the microstructural evolution and mechanical properties without focusing on the resulting shape memory properties such as transformation and/or irrecoverable strain levels.

The present work compares the effects of ECAE and cold drawing followed by low temperature annealing on the cyclic stability of transformation response and thermal hysteresis in the $Ti_{50.27}Ni_{49.73}$ alloy. SPD via ECAE was performed isothermally at a relatively low temperature (300 °C). The results showed that ECAE is a viable method to improve the thermal cyclic stability and to decrease the thermal hysteresis under higher stress levels in NiTi.

## 2. Experimental procedure

A NiTi alloy with a nominal composition of 50.27 at.% Ti and 49.73 at.% Ni was acquired from Special Metals Corporation, New Hartford, New York. The as-received material was cold-drawn to 30%. The initial material was then solutionized at 1000 °C for 1 h in an evacuated quartz tube and quenched in water prior to ECAE. NiTi bar with 12 mm diameter and 100 mm length was canned in pure nickel with $25.4 \times 25.4\ mm^2$ square-shaped cross-section and 150 mm length. To fabricate the Ni can, a hole with 12 mm diameter and 125.4 mm length was drilled in a $25.4 \times 25.4\ mm^2$ cross-section, 150 mm long Ni bar. After placing the NiTi bar in the can, a pure Ni plug with the same diameter and 25.4 mm length was inserted into the can. The reason for encapsulating NiTi was to eliminate the friction between the billet and the ECAE tool and to protect the tool from unexpected strain hardening in NiTi. The canned sample was heated to 300 °C and held for 1 h prior to extrusion. ECAE was performed isothermally in the tool with the die angle of 90°. One ECAE pass in a tool with sharp 90° corner angle was shown to correspond to the equivalent strain level of 1.15 and equivalent area reduction of 69% [4]. The extrusion rate was 0.25 mm/s. The extruded billet was quenched in water after extrusion to maintain the microstructure achieved during ECAE and the NiTi bar was extracted from the can. Fig. 1 shows the appearance of the extracted bar which has the expected sheared shape after one ECAE pass. This result demonstrates that NiTi has sufficient ductility for ECAE processing at temperatures low enough to prevent

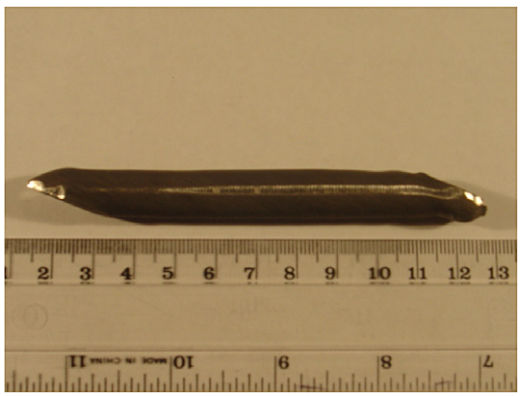


Fig. 1. The digital image of the $Ni_{49.73}Ti_{50.27}$ bar which was ECAE processed isothermally at 300 °C with an extrusion rate of 0.25 mm/s.

dynamic recrystallization. Note that the material's structure was martensite during cold-drawing (thus, the process is called marforming), while ECAE was conducted in austenite (i.e. ausforming). Some of the as-received materials were annealed at 300 °C for 30 min to investigate the influence of cold work followed by low temperature annealing process. We performed differential scanning calorimetry (DSC) to determine the transformation temperatures of the as-received, solutionized, low temperature annealed and ECAE-processed materials with a heating–cooling rate of 10 °C/min.

Small dog-bone shaped tension specimens were cut using wire electro-discharge machining (EDM). The gauge section of the samples was $1 \times 3 \times 8\ mm^3$. The specimens were subjected to thermal cycles under the stress levels of 100 and 200 MPa. All mechanical tests were performed using an MTS servo-hydraulic test frame. The axial strain was measured using a miniature extensometer with a 3 mm gauge length and a maximum working temperature of 200 °C. The heating/cooling of the samples was achieved by conduction through the grips which were heated by heating bands and cooled by liquid nitrogen flowing through copper tubing wrapped around the grips, with a heating/cooling rate of 10 °C/min. The temperature was measured using thermocouples directly attached to the samples.

Transmission electron microscopy studies were conducted using a JEOL 2010 microscope operated at an accelerating voltage of 200 kV. TEM foils were prepared by mechanical grinding down to 100 μm and then polished using twin-jet electropolisher with a 20 vol.% $H_2SO_4$ and 80 vol.% methanol solution at −10 °C.

## 3. Results and discussion

### 3.1. DSC analysis

DSC responses of the cold-drawn, solutionized, cold-drawn and annealed, and ECAE processed samples are shown in Fig. 2. Each curve in the figure consists of three heating–cooling cycles. No transformation was detected in the cold-drawn sample at temperatures as low as −60 °C, however annealing at 300 °C for 30 min led to increase in the transformation temperatures due to the recovery of unstable dislocation structures.

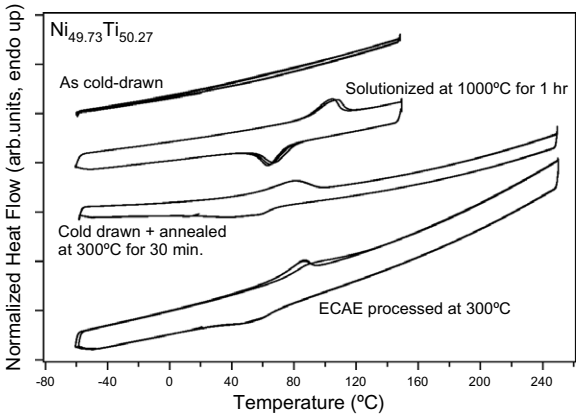


Fig. 2. DSC response of the solutionized, cold-drawn, cold-drawn and annealed, and ECAE processed $Ni_{49.73}Ti_{50.27}$ alloy.

The phase transformation temperatures (austenite finish ($A_f$), austenite start ($A_s$) martensite start ($M_s$), and martensite finish ($M_f$)) and four additional parameters ($A_f$–$M_f$, $A_f$–$M_s$, $A_f$–$A_s$, and $M_s$–$M_f$) are determined from the DSC results and summarized in Table 1. The first parameter ($A_f$–$M_f$) is an indication of the combined effect of stored elastic energy and energy dissipation during forward and reverse phase transformations. The second parameter ($A_f$–$M_s$) only demonstrates the significance of energy dissipation which is related to frictional work and spent for overcoming the resistance to interfacial motion [16]. For the cold-drawn and annealed case, $A_f$–$M_f$ is 87 °C while $A_f$–$M_s$ is 28 °C. These values are higher than those of the ECAE processed sample listed in Table 1. These parameters depend on the processing conditions and the higher values in the cold-drawn and annealed sample are probably due to the difficulty of phase front motion in the presence of remnant dislocation structure. It is obvious from the table

Table 1
Summary of the transformation temperatures determined from the DSC responses shown in Fig. 2

| Processing conditions | $M_s$ (°C) | $M_f$ (°C) | $A_s$ (°C) | $A_f$ (°C) | $A_f$–$M_s$ (°C) | $A_f$–$A_s$ (°C) | $A_f$– $M_f$ (°C) | $M_s$–$M_f$ (°C) |
|---|---|---|---|---|---|---|---|---|
| Solutionized | 78 | 54 | 87 | 115 | 37 | 28 | 61 | 24 |
| Cold-drawn + annealed at 300 °C | 69 | 10 | 49 | 97 | 28 | 48 | 87 | 59 |
| One pass ECAE at 300 °C | 72 | 28 | 61 | 94 | 22 | 33 | 66 | 44 |

that cold deformation decreased all transformation temperatures. For the cold-drawn and annealed sample, $A_f$–$M_s$ value is lower but $A_f$–$M_f$ value is higher than those for the solutionized case. This means that cold deformation changes the microstructure of the material such that elastic stored energy during transformation increases and the dissipation of the stored energy during phase front motion (through detwinning or dislocation accommodation at the interface) decreases. Increase in elastic stored energy and decrease of its dissipation, in turn, cause the decrease in $M_f$, $A_f$ and $A_f$–$M_s$ [16]. For practical concerns and cyclic transformation response, one needs sufficiently large elastic strain energy storage and small energy dissipation such that $A_f$–$M_s$ would be small but at the same time $M_f$ would not be too low. However, cold deformation seems to cause a decrease in $A_f$–$M_s$ but at the same time leads to a large drop in $M_f$.

Similar to the cold-drawn case, ECAE decreases both the $A_f$ and $M_s$ temperatures as compared the solutionized case. The $M_f$ temperature was also dropped in the ECAE processed sample, however, the effect was not as significant as in the cold-drawn and annealed sample. As far as the thermal hysteresis is concerned, ECAE processing decreased the $A_f$–$M_s$ significantly down to 22 °C, the lowest value among all the cases. Moreover, $A_f$–$M_f$ is also considerably lower than that of the cold-drawn and annealed sample. The high $A_f$–$M_f$ value in the latter case is the indication of large transformation temperature interval to complete the transformation and also related to the competition between the amount of elastic strain energy storage plus the way it is stored and the elastic strain energy dissipation. This issue has been discussed in detail in the following section.

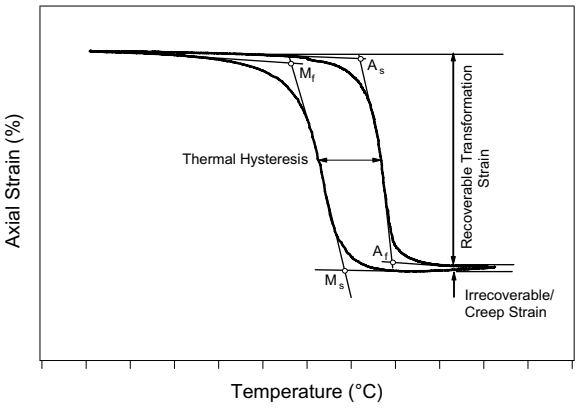


Fig. 3. A schematic of the strain vs. temperature response of a SMA sample under constant stress showing the definitions of the parameters used in the present study.

### 3.2. Isobaric thermal cycling

Thermal cycling tests up to 10 cycles were conducted between a temperature below $M_f$ and a temperature above $A_f$ under 100 and 200 MPa. The main purpose of these experiments was to evaluate thermal hysteresis evolution, recoverable transformation and irrecoverable/creep strain levels as a function of the number of cycles. These parameters are schematically defined in Fig. 3. The response of the cold-drawn and annealed sample is shown in Fig. 4. The as-received cold-drawn sample response was not shown since the transformation temperatures were low and 200 MPa stress level was not sufficient to capture a complete transformation

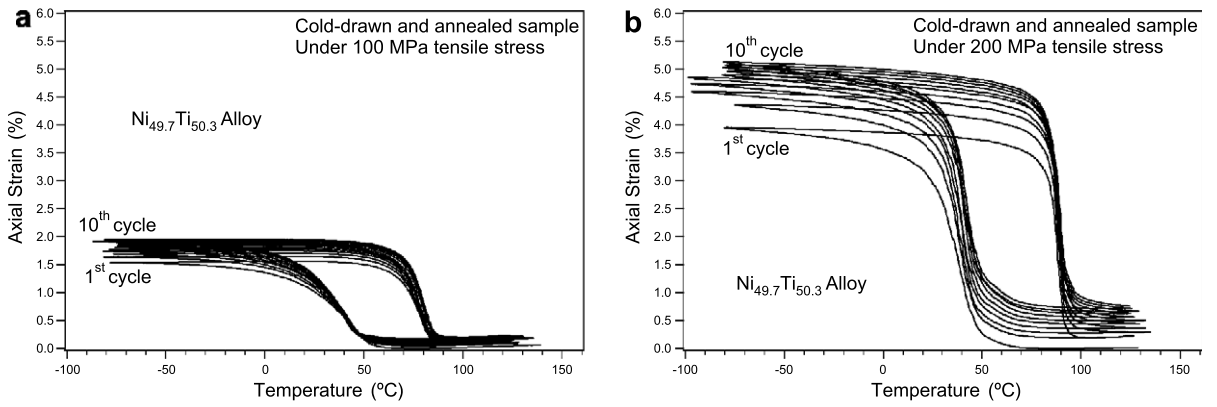


Fig. 4. The strain vs. temperature response of the cold-drawn and low temperature annealed (at 300 °C for 30 min) $Ni_{49.73}Ti_{50.27}$ samples under (a) 100 MPa and (b) 200 MPa.

cycle above −100 °C. Note that the purpose of the annealing at 300 °C was to slightly recover the microstructure such that the less stable dislocations are annealed out and the more stable ones are maintained causing transformation temperatures to increase. The annealing temperatures higher than 400 °C usually result in considerable recovery and some recrystallization in NiTi alloys.

The annealed sample shows a total irrecoverable strain of 0.75% and a total transformation strain of 4% after 10 cycles under 200 MPa. An interesting feature in the strain vs. temperature response is the change in thermal hysteresis as a function of martensite volume fraction. It is observed that the hysteresis becomes wider with increasing transformation strain level. This shows that the forward transformation requires large undercooling to complete the transformation probably because of the difficulty of phase front motion in the presence of relatively stable dislocation substructures.

Fig. 5 exhibits the cyclic strain vs. temperature response of the ECAE processed samples under 100 and 200 MPa. The transformation strain under 100 MPa is initially 1.25% and then increases and stabilizes at around 1.5%. The total irrecoverable strain after 10 cycles is 0.19% under 100 MPa. Under 200 MPa it does not change much and becomes only 0.21%. The transformation strain is 3.5% under 200 MPa.

Fig. 6 shows the evolution of the transformation and total irrecoverable strain levels as a function of the number of cycles for both cases. The transformation strain at each stress level for the ECAE processed sample is lower than that for the cold-drawn and annealed sample. This was expected because the ECAE processed sample should be stronger due to the much higher deformation level applied [4,17]. In other words, the critical stress level for the onset of phase transformation is higher, and thus, higher external stresses need to be applied for obtaining

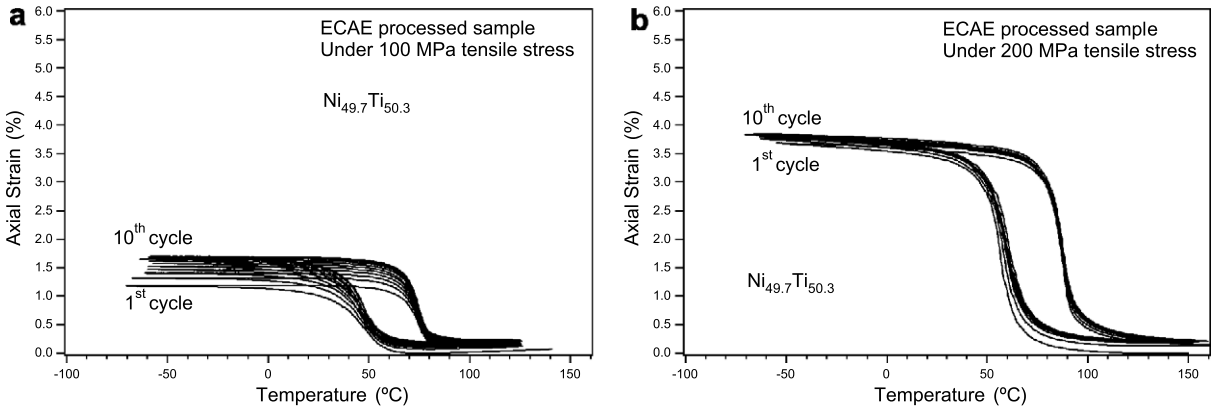


Fig. 5. The strain vs. temperature response of the one pass ECAE processed samples at 300 °C under (a) 100 MPa and (b) 200 MPa.

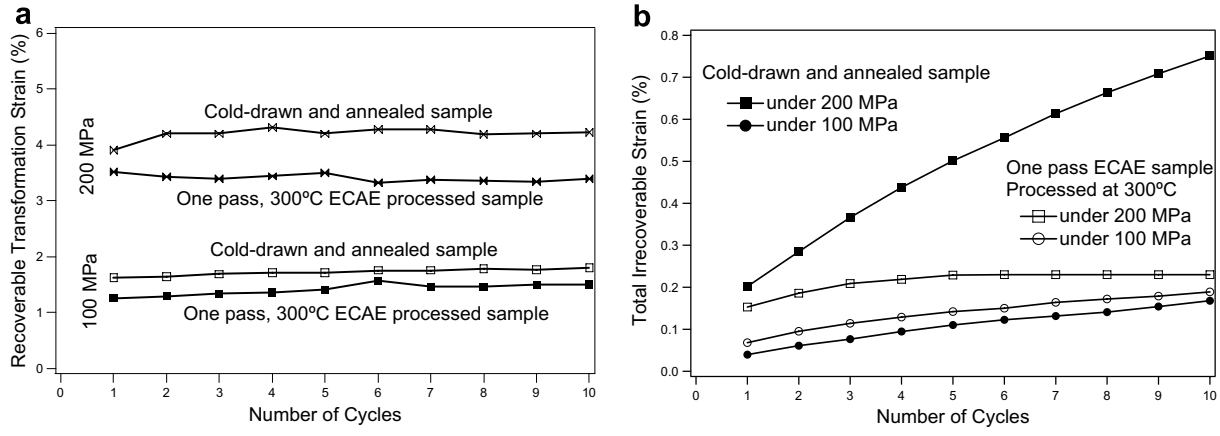


Fig. 6. (a) Recoverable transformation and (b) accumulated irrecoverable strain response of the ECAE processed (one pass at 300 °C) and cold-drawn plus annealed samples as a function of the number of thermal cycles under 100 and 200 MPa.

maximum transformation strain level available in NiTi. The total irrecoverable strain is not much different than that of the cold-drawn and annealed sample at the lower stress, but under 200 MPa there is a significant improvement (decreased irrecoverable strain) in the ECAE case. Such improvement can be attributed to the strengthening effect such that dislocation generation partially accommodating phase transformation, thus dissipation of the stored elastic energy, is more difficult in the ECAE processed sample. It is believed that the low temperature annealing would decrease the irrecoverable strain further in the ECAE processed sample as observed in a NiTiHf alloy after ECAE and low temperature annealing [18]. This expectation stems from the possibility of further strengthening in the material due to polygonization and/or vacancy/interstitial pair formation.

Fig. 7(a) and (b) shows the bright and dark field TEM images of the ECAE processed sample taken at 200 °C exhibiting deformation twinning in austenite. The microstructure is heavily deformed with high dislocation density and significantly refined with relatively high volume fraction of twins having thicknesses in the nanometer range. Fig. 7(c) and (d) demonstrates that the matrix is B2 austenite and the elongated features are twins. The twinning plane is determined as $(1\,\bar{3}\,1)$ which is one of the common twinning planes observed in B2 NiTi. The improvement in the thermal cyclic stability under high stress levels in the ECAE processed sample is, thus, attributed to the strengthening of the material due to this refined microstructure and nanometer range deformation twins.

An intriguing finding, when comparing the thermal cycling responses of the cold-drawn plus

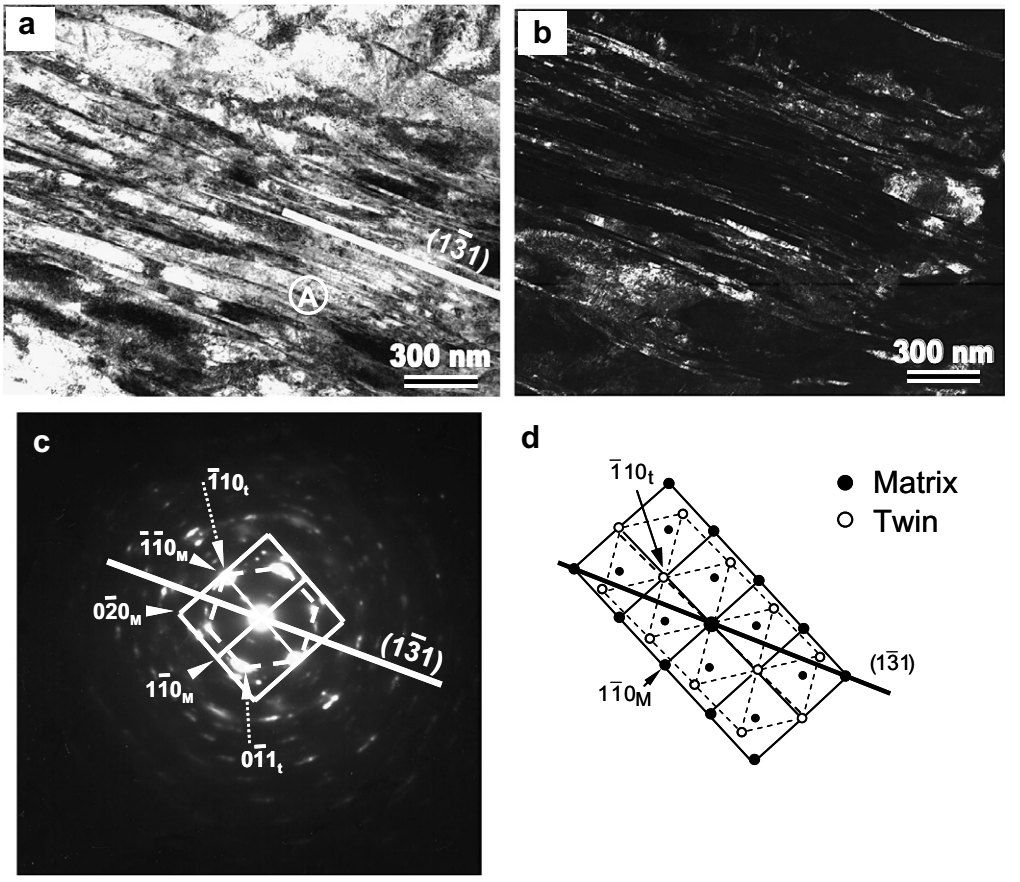


Fig. 7. TEM images of the near equiatomic NiTi after one ECAE pass at 300 °C showing deformation twins in austenite at 200 °C: (a) bright field and (b) dark field images of twins. (c) Electron diffraction pattern from region A in (a). (d) Schematic diagram of matrix and twin lattices shown in (c). Twin zone axis is [1 1 1], the matrix (parent phase) zone axis is [0 0 1], and twinning plane is $(1\,\bar{3}\,1)$. The dark field image in (b) was taken from $(0\,\bar{1}\,1_t)$.

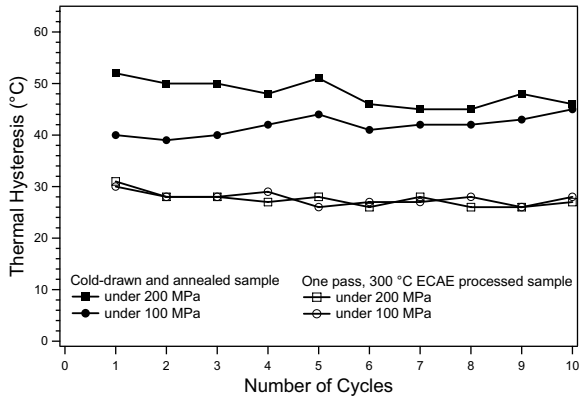


Fig. 8. Thermal hysteresis as a function of the number of thermal cycles during isobaric thermal cyclic experiments under 100 and 200 MPas.

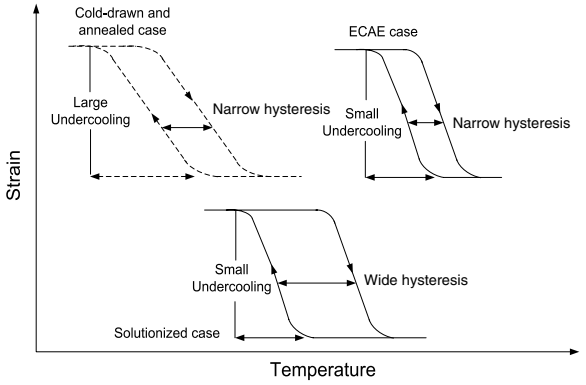


Fig. 9. A schematic demonstrating the effect of elastic stored energy, undercooling, and energy dissipation on the thermal cyclic response of SMAs under constant stress levels for three different cases mentioned in the text.

annealed and ECAE processed samples, is the considerable decrease in the thermal hysteresis of the ECAE processed samples (Fig. 8). Moreover, the thermal hysteresis does not increase with the applied stress level in the latter case although a considerable increase would be expected as in the case of the cold-drawn and annealed sample. Thermal hysteresis in NiTi originates from the accommodation of martensitic transformation shear with martensite internal twins and dislocation formation at the phase boundary instead of the elastic distortion of the matrix. When the stress levels are increased, dislocation formation, and thus irreversible energy dissipation, becomes easier and thermal hysteresis increases. If the material is strengthened either by ausforming, marforming or precipitation hardening, the stress required for new dislocation formation increases. Thus, the increase in the strength upon ECAE and the effect of such strengthening on the competition between the storage and dissipation of elastic strain energy is the main cause for the anomaly in the thermal hysteresis of the ECAE processed samples.

From our current observations on NiTi and previous observations on NiTiHf [18], it appears that ECAE processing can improve cyclic stability under stress and decrease the thermal hysteresis. To better understand the mechanisms responsible for such improvements, it is necessary to discuss the factors affecting the shape of the thermal cyclic response under constant stress levels and the correlation with the elastic energy storage and the irreversible energy dissipation upon phase transformation. The schematic illustration shown in Fig. 9 elucidates how stored elastic strain energy evolution determines the transformation temperature interval (i.e. $M_s$–$M_f$), hence changing the cooling slope of the strain vs. temperature curve. When the stored elastic strain energy is high, the slope of the curve is shallow ($M_s$–$M_f$ is high as in the case of cold-drawn and annealed NiTi), whereas when the stored energy is low, the slope of the curve is steep ($M_s$–$M_f$ is low as in the case of solutionized NiTi – not shown here). One of the reasons for the observed low elastic stored energy is the dissipation of stored elastic energy during the phase front motion, especially with increasing stress level, which might be a consequence of dislocation activity under high stresses [16,19]. Increasing energy dissipation naturally leads to larger thermal hysteresis, i.e. the higher the $A_f$–$M_s$. Thus, one can argue that the higher the stored elastic strain energy, the lower the heating necessary to initiate reverse transformation, and the lower the $A_f$–$M_s$. Therefore, there is an inverse relationship between $A_f$–$M_s$ and $M_s$–$M_f$, as observed in comparing the transformation behavior of cold-drawn and annealed samples with that of the solutionized one (Table 1, Figs. 4 and 8). The results from Hamilton et al. [16] on NiTi single crystals also support this argument. On the other hand, it seems that the ECAE sample does not follow this trend as both parameters decreases as compared to the cold-drawn and annealed sample. This is probably related to increased resistance against energy dissipation.

Preferred austenite texture formation near [1 0 0] pole can suppress dislocation generation considerably, and thus, decrease energy dissipation during phase transformation since the possible slip systems in these alloys are $\{110\}\langle001\rangle$ and $\{100\}\langle001\rangle$ [20,21]. However, since the $A_f$ temperature is relatively high in the present case, it was not possible

to measure the austenite texture with conventional means to prove the existence of such texture in the ECAE sample. Formation of refined microstructure due to very fine deformation twins may also help suppressing energy dissipation while it may not affect the transformation temperature interval (energy storage) significantly. Deformation twin boundaries in austenite or compound twin boundaries in martensite are shown to transform into twin boundaries in martensite or vice versa [13,22]. Thus these boundaries do not affect elastic energy storage and undercooling requirement as much as a typical grain boundary or dislocation cell walls do. On the other hand, the material is stronger due to these twins making new dislocation generation and energy dissipation more difficult, and as a result, the thermal hysteresis is narrower.

## 4. Conclusions

The following conclusions can be drawn from the present study:

(1) It is possible to isothermally process near-equiatomic NiTi alloys at temperatures as low as 300 °C using ECAE without macroscopic shear localization.
(2) ECAE processing at 300 °C significantly decreased the thermal hysteresis and improved the cyclic stability (decreased irrecoverable strain) of the NiTi as compared to cold drawing plus low temperature annealing. This was attributed to the microstructural refinement due to the formation of very fine deformation twins in austenite during ECAE which led to the strengthening of the material via increase in the critical shear stress for slip and thus, suppressing the dissipation of stored elastic energy during martensitic phase transformation.
(3) As the applied stress level increases, the decrease in thermal hysteresis and the improvement in the cyclic stability in the ECAE processed sample become more pronounced.

## Acknowledgement

This work was supported by the US Office of Naval Research. Contract No. N00014-03-M-0332 and Marlow Industries Inc.

## References

[1] K. Otsuka, C.M. Wayman, Shape Memory Materials, Cambridge University, Cambridge, 1999.
[2] A. Okada, K. Hamada, T. Matsumoto, I. Ishida, Y. AbeA, J. Nucl. Mater. 271&272 (1999) 189.
[3] M. Nishikawa, M. Kawai, T. Yokoyama, T. Hoshiya, M. Naganuma, M. Kondo, K. Yoshikawa, K. Watanabe, J. Nucl. Mater. 179–181 (1991) 1115.
[4] V.M. Segal, Mater. Sci. Eng. A 197 (1995) 157.
[5] R.Z. Valiev, R.K. Islamgaliev, I.V. Alexandrov, Progr. Mater. Sci. 45 (2000) 103.
[6] R.S. Misra, R.Z. Valiev, S.X. Macfadden, A.K. Mukherjee, Mater. Sci. Eng. A 252 (1998) 174.
[7] R.Z. Valiev, A.K. Mukherjee, Scripta Mater. 44 (2001) 1747.
[8] Y. Liu, G.S. Tan, Intermetallics 8 (2000) 67.
[9] Y. Liu, D. Favier, Acta Mater. 48 (2000) 3489.
[10] D.A. Miller, D.C. Lagoudas, Mater. Sci. Eng. A 308 (2001) 161.
[11] A.V. Sergueeva, C. Song, R.Z. Valiev, A.K. Mukherjee, Mater. Sci. Eng. A 339 (2003) 159.
[12] V.G. Pushin, V.V. Stolyarov, R.Z. Valiev, T.C. Lowe, Y.T. Zhu, Mater. Sci. Eng. A 410&411 (2005) 386.
[13] I. Karaman, A. Kulkarni, ZP. Luo, Philos. Mag. 85 (2005) 1729.
[14] V.G. Pushin, R.Z. Valiev, Solid State Phen. 94 (2003) 13.
[15] V.G. Pushin, V.V. Stolyarov, R.Z. Valiev, N.i. Kourov, N.N. Kuranova, E.A. Prokof'ev, L.I. Yurchenko, Phys. Met. Metall. 94 (2002) S54.
[16] R.F. Hamilton, H. Sehitoglu, Y. Chumlyakov, H.J. Maier, Acta Mater. 52 (2004) 3383.
[17] V.G. Pushin, V.V. Stolyarov, R.Z. Valiev, T.C. Lowe, Y.T. Zhu, Mater. Sci. Eng. A 410 (2005) 386.
[18] B. Kockar, I. Karaman, J.I. Kim, Y. Chumlyakov, Scripta Mater. 54 (2006) 2203.
[19] K. Wada, Y. Liu, Smart Mater. Struct. 14 (2005) S273.
[20] N.S. Surikova, Y.I. Chumlyakov, Fiz. Met. Metalloved 89 (2000) 98.
[21] E. Hornbogen, G. Bruckner, G. Gottstein, Z. Metallkd. 93 (2002) 3.
[22] S. Ii, K. Yamauchi, Y. Maruhashi, M. Nishida, Scripta Mater. 49 (2003) 723.